17th World Conference on Earthquake Engineering, 17WCEE
Sendai, Japan - September 13th to 18th 2020
Paper N° C001526
Registration Code: S-A02536

EFFECT OF AN INNOVATIVE ISOLATION SYSTEM ON THE SEISMIC RESPONSE OF CULTURAL HERITAGE BUILDING CONTENTS

G. Guerrini[(1)], U. Tomassetti[(2)], F. Graziotti[(3)], M. Rota[(4)], A. Penna[(5)],

[(1)] *Post-doctoral researcher, University of Pavia and EUCENTRE Foundation, gabriele.guerrini@unipv.it*
[(2)] *Post-doctoral researcher, University of Pavia, umberto.tomassetti01@universitadipavia.it*
[(3)] *Assistant professor, University of Pavia and EUCENTRE Foundation, francesco.graziotti@unipv.it*
[(4)] *Researcher, EUCENTRE Foundation, maria.rota@eucentre.it*
[(5)] *Associate professor, University of Pavia and EUCENTRE Foundation, andrea.penna@unipv.it*

Abstract

An experimental study was conducted at the University of Pavia and at the EUCENTRE Foundation (Pavia, Italy) to assess the effectiveness of an innovative seismic isolation device at protecting cultural heritage building contents. The recently patented isolator, named "Kinematic Steel Joint (KSJ)", is based on a multiple articulated quadrilateral mechanism and is entirely made of steel components obtained by simply cutting, folding, and pinning metal sheets, eventually employing stainless steel to limit corrosion issues. The trajectory imposed by the KSJ isolator to the supported mass combines horizontal with increasing vertical displacements, resulting in a pendulum-type motion with self-centering behavior. The friction developing within the pinned joints can be exploited to grant energy dissipation capacity to the device. The KSJ isolator can be manufactured with different sizes, payloads, and displacement ranges. In fact, seismic isolation can be applied at a global building level as an integrated system or as a retrofit solution in new or existing construction, respectively, or at a local scale as a passive protection technique for non-structural components. Despite their undeniable effectiveness in reducing the seismic accelerations transmitted to the isolated structure and to its content, currently available isolation devices may add significantly to the construction cost of buildings, and may require particular maintenance to preserve a stable performance over time. The proposed KSJ solution will allow for a reduction in manufacturing and maintenance burdens compared to established technologies.

This paper discusses the main results of a shake-table test conducted at the EUCENTRE Foundation laboratories on an assembly with four prototypes of the KSJ device. The experimental setup included a 19-t rigid mass supported by the isolators, simulating the building superstructure, and four marble blocks installed above the rigid mass, representing non-structural rocking components such as parapets, pinnacles, statues, or other architectural ornaments. Moreover, a museum showcase with a small-scale replica of Michelangelo's David was mounted above the rigid block, while two clay vases completed the setup, to encompass additional cultural heritage features. Accelerometers and potentiometers were deployed at several locations to monitor the kinematic response of the individual isolators, as well as their effect on the dynamic response of the rigid mass and of the different non-structural elements. The experiment was conducted first with the KSJ devices allowed to displace freely, then after fastening the rigid mass to the shake-table through post-tensioning rods, following the same incremental dynamic test sequence. This allowed comparing the response of the non-structural components with and without seismic isolation, to better understand the effect of the proposed isolation devices on the overall test assembly and on each sub-component.

Keywords: cultural heritage, kinematic steel joint, non-structural components, seismic isolation, shake-table test

1. Introduction

Earthquake-induced cyclic accelerations on buildings can cause damage to structural and non-structural components, eventually leading to partial or total collapse. The current seismic design philosophy focuses on the concept of structural ductility, i.e. on the ability of structures to deform beyond their elastic limit: the development of extensive damage is accepted as long as collapse is prevented [1]. However, protecting buildings from earthquakes requires not only to ensure life safety and collapse prevention, but also to limit the economic and social cost of post-event disruption, repair, and reconstruction. This is particularly true when valuable contents are to be preserved, such as cultural heritage, technological, or hospital assets [2]–[6]. For this reason, seismic isolation technologies have been slowly establishing alongside the more traditional ductile design approach over the past few decades.

Seismic isolation acts as a filter for the seismic input transmitted to the superstructure (the entire building or a portion of it) above the isolation layer, to reduce the acceleration, displacement, and deformation demand imposed on its elements and on its contents, and the potential damage to structural and non-structural components. Seismic isolation can be integrated in new buildings from construction, or added to existing buildings as a seismic retrofit solution. Typically, it is provided at the basement level or crawl space of buildings, from which the widespread definition of "base isolation", even though seismic isolation may be alternatively suitable at higher locations, depending on the building configuration or on which portions require special protection [7]. Isolation can be limited also to specific building areas: for example, floating floors supported on seismic isolators can be installed only in selected rooms [8]–[9], to decouple their movements from structural accelerations and protect valuable contents. In some instances, individual non-structural elements can be isolated from ground or floor accelerations [10]–[15].

A typical base isolation system, schematically represented in Fig. 1, first needs to possess low lateral stiffness, to decouple the ground motion from that of the horizontal rigid diaphragm located at the superstructure base. The second essential requirement is its ability to dissipate energy, to limit the deformation demand on the isolators themselves. Finally, the isolation system needs to recenter to its at-rest position at the end of the seismic excitation. All these features can be found in individual elastomeric and friction pendulum bearings, which are mostly adopted as isolators for building structures. Isolators, based on other principles such as rollers or suspension systems, are also available and can provide satisfactory performance in combination with independent energy dissipators and recentering devices [16].

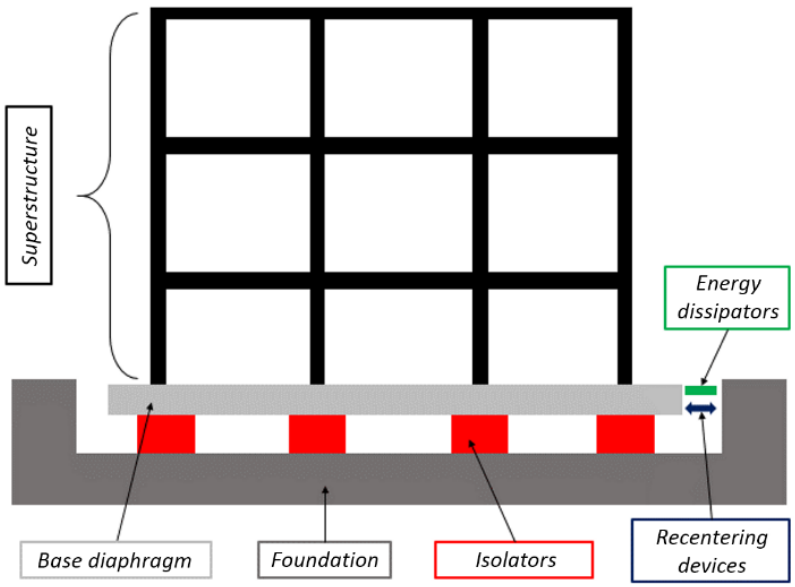

Fig. 1 – Schematic seismic isolation system.

Seismic isolation can significantly increase the construction cost of ordinary buildings in some cases, making this technology less appealing for their owners. Moreover, isolation devices may need specific maintenance or replacement over time, to control elastomer aging, steel corrosion, sliding surface degradation, and other effects that may impair their performance [17]–[21]. Consequently, access to the isolators and energy dissipators must be granted even when they are located within crawl spaces.

To address the issues above, Kyneprox S.r.l. has patented a new type of isolator, consisting of a double articulated quadrilateral with crossing rods entirely made of steel, named "Kinematic Steel Joint" (KSJ). Stainless steel can be used for practical implementations, to reduce corrosion sensitivity. The device imposes a recentering pendulum-type motion to the superstructure, as it associates horizontal with upward displacements. Similarly to friction pendulum isolators, the restoring force is proportional to the slope of the trajectory. The KSJ also provides some energy dissipation, due to friction within pin connections between its members. The device can be produced with different sizes, payloads, and displacement capacities, making it suitable for a variety of applications ranging from non-structural content to entire building isolation.

This paper discusses the main results of a shake-table test conducted at the EUCENTRE Foundation laboratories on an assembly with four KSJ devices, a rigid mass simulating the building superstructure, and several components representing cultural heritage assets.

2. KSJ prototype features

Fig. 2 shows the KSJ prototype considered in this study. The prototype was made of S235 steel rods and plates, because durability was not an issue for the experimental campaign. However, stainless steel would be used for commercial devices to tackle corrosion issues. Connections between members consisted of bolts and thrust bearings, acting as pins with some frictional resistance.

Top and bottom square plates, with 10-mm thickness and 400-mm side, allowed connecting the device to the shake-table (foundation) and to the rigid mass (superstructure) by four 16-mm diameter bolts each. Three rows of 10-mm-thick vertical plates, with shape compatible with the pendulum-type motion of the rods and with their maximum rotations, were fillet-welded to the horizontal plates. Three modules, each consisting of four diagonal rods crossing in pairs and a horizontal rod, were mounted side by side in parallel and pinned to the vertical plates. All rods were obtained from 10-mm-thick steel sheets; notches and chamfers allowed to accommodate the maximum rod rotations corresponding to the displacement capacity of the device.

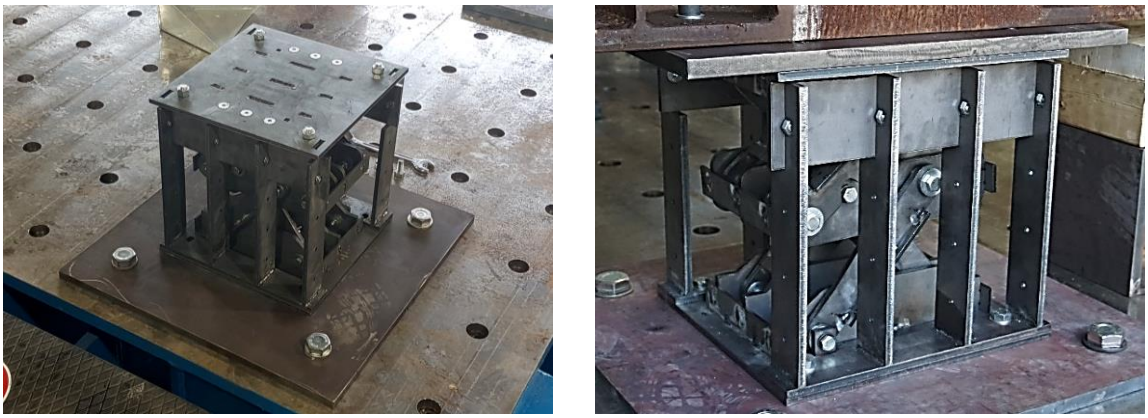

Fig. 2 – Kinematic Steel Joint (KSJ) isolator prototype.

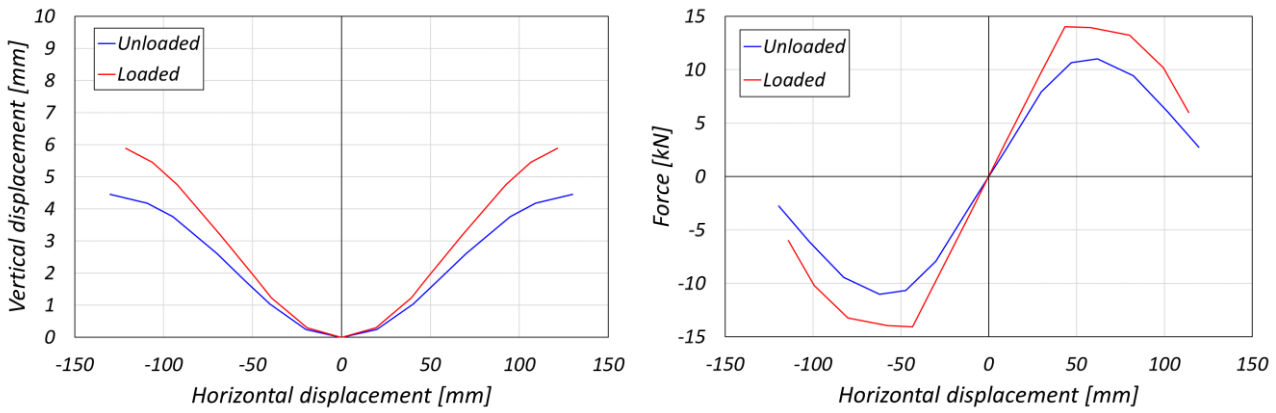

(a) (b)

Fig. 3 – Analytical response of the KSJ prototype: (a) trajectories of an individual device; (b) lateral force-displacement envelopes for a superstructure weight of 205 kN [22].

A restraining system, consisting of rigid steel plates and cylindrical bearings, forced the device horizontal displacement in a single direction, preventing transverse and torsional deviations. For practical applications, combining two devices with orthogonal orientation on top of each other would allow full 2-dimensional motion in a horizontal plane. Aligning more than one KSJ isolators, fixed to the shake-table and to the rigid superstructure mass, prevented the rotation of the top horizontal plate and resulted in a single-degree-of-freedom (SDOF) system with pendulum-type motion. The same result can be obtained in applications to buildings, providing sufficient out-of-plane flexural stiffness to the base horizontal diaphragm.

An analytical study was performed on the device to establish its kinematic, static, and dynamic properties [22]. In particular, a variable-curvature trajectory characterizes the KSJ kinematic behavior, with restoring force proportional to the local slope, and lateral stiffness proportional to the local curvature. The average radius of curvature R, for a given lateral displacement along the trajectory, is defined as the radius of the circle through the at-rest position and through the symmetrical points at the positive and negative displacement of interest. The average period T_b of the isolated system (assumed rigid) is obtained from the average radius R as for a simple pendulum, independently of the mass. Moreover, geometric variations due to gravity loading affect the lateral response of the KSJ isolator. In fact, the maximum horizontal displacement slightly reduced from ±130 mm to ±121 mm, while the trajectory became steeper and the lateral stiffness increased. Consequently, the average isolation period at 80-mm lateral displacement reduced from 2.1 s to 1.8 s. Fig. 3 shows the analytical trajectories and lateral force-displacement envelopes for the KSJ prototype under unloaded and loaded geometric conditions.

3. Dynamic shake-table test

3.1 Test setup

A unidirectional (North-South) dynamic shake-table test was conducted at the 6DLab of the EUCENTRE Foundation in Pavia, Italy, to investigate the behavior of the KSJ prototype experimentally. The setup included four in-parallel devices, supporting a mass with a total weight of 205 kN (Fig. 4). Two steel guides were mounted below the longitudinal beams to prevent transverse (East-West) and torsional motion, should the out-of-plane restraints of the devices have failed. Two safety steel braces were provided to stop the mass in case of failure of the KSJ devices or of their connections, after reaching the maximum longitudinal displacement capacity.

(a) (b)

Fig. 4 – Shake-table test setup: (a) isolated configuration; (b) fixed-base configuration.

The main contribution to the mass came from a 158-kN reinforced concrete (RC) prismatic block, resting above two longitudinal HE 400 B steel beams (10.1 kN each), which in turn were supported by two KSJ isolators each. Four steel adaptor plates connecting isolators and beams provided additional 0.4 kN each. Among the non-structural elements, a museum showcase provided by Goppion S.p.A. (2.5 kN) was fastened above the main RC mass. The showcase contained a small-scale, 3D-printed replica of Michelangelo's David statue with negligible mass. Two clay vases (negligible mass), supported by two 2.3-kN concrete blocks, were arranged on the main mass next to the showcase.

Non-structural elements included also marble blocks to simulate rocking heritage components. A 1.55-m-tall block, with horizontal cross-section of 0.315 x 0.315 m (4 kN), resting on a conic base (2.6 kN) attached to the RC mass, simulated a statue allowed to rock in any direction. This block, identified in the following as "free-rocking block", had semi-diagonal of 0.791 m and slenderness angle with tangent equal to 0.203. A second, 1.55-m-tall block, with cross-section of 0.16 x 0.63 m (4 kN), was forced to rock on one side only by a perpendicular block (8 kN) fixed to the main mass. This component, termed "one-side-rocking block", was characterized by semi-diagonal of 0.779 m and slenderness angle with tangent equal to 0.103.

Before the dynamic test, a quasi-static test was conducted to assess the force-displacement relationship of the setup. The same setup was used, except that the mass was tied to the laboratory strong-floor by a steel cable (visible in Fig. 4a) with a load cell, which were then removed to proceed with the dynamic test phase. Two series of dynamic fixed-base tests were also performed after fastening the concrete mass to the steel braces (Fig. 4b), to evaluate the response of the non-structural components in this condition. Only horizontal accelerations were applied in the first fixed-base test series, while the second sequence included the vertical ground-motion component.

3.2 Instrumentation layout

All components of the setup were instrumented with accelerometers, potentiometers, and wire potentiometers. Among others, one triaxial accelerometer was mounted at the center of the shake-table platen, and two triaxial accelerometers were provided at the East and West sides of the reinforced concrete block (visible in Fig. 4a). The overall inertial force of the system was determined by associating 50% of the total mass with each instrument on the block. Triaxial accelerometers were attached to each moving marble block, while uniaxial sensors were provided to the conic base and to the fixed block. Uniaxial accelerometers were also mounted on the showcase, on the David statue, and on the support of the David statue.

Potentiometers were used to record the motion of the isolators. In particular, each KSJ device was monitored by three potentiometers along three orthogonal directions (Fig. 5a): two of them were necessary to recover the pendulum-type trajectory within the vertical plane, while the third one allowed verifying the

efficiency of the out-of-plane restraint at preventing transverse displacements. A pair of potentiometers was also employed to check that no sliding occurred between reinforced concrete block and steel beams. Two wire potentiometers recorded the displacements of the rocking marble blocks (Fig. 5b).

3.3 Test protocol

The incremental dynamic test was conducted applying two natural-seismicity ground-motion records to the shake-table. The records were downloaded from the Italian database ITACA (ITalian ACcelerometric Archive) [23], provided by the National Institute of Geophysics and Volcanology. The first signal, labeled EMN, was recorded during the 2012 Northern Italy earthquake sequence; the second one, abbreviated CIN, during the 2016 Central Italy seismic events. More details can be found in Table 1.

For the base-isolated test series, only the horizontal component of each record was applied, scaling its acceleration amplitude at 25%, 50%, 75%, 100%, 125%, 150%, 175%, 200%, and 250%. In the first fixed-base test sequence, the EMN record was scaled only up to 200%, while the CIN input only up to 125%, to avoid irreversible damage to the showcase. The second fixed-base test series included the vertical ground-motion component, scaled by the same factor used for the horizontal one. In this test sequence, the maximum scale factors were 175% for EMN and 150% for CIN.

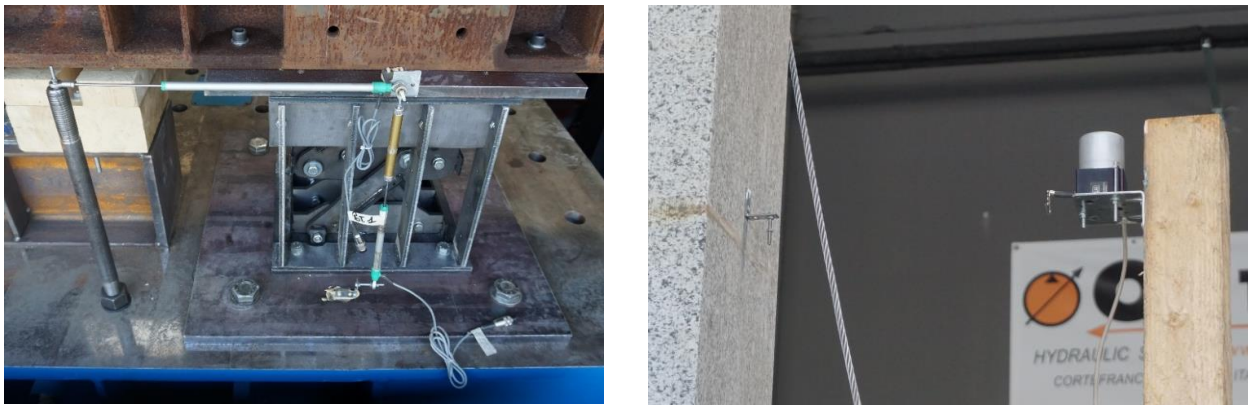

(a) (b)

Fig. 5 – Instrumentation layout: (a) potentiometers for isolator trajectories; (b) wire potentiometer for free-rocking block displacements.

Table 1 – Input signal characteristics.

Parameter	EMN	CIN
Date	29/05/2012	30/10/2016
Time	06:40:18	07:00:02
Moment magnitude	6.0	6.5
Province	Modena	Perugia
Municipality	Finale Emilia	Preci
Latitude [°]	44.8486	42.8793
Longitude [°]	11.2479	13.0334
Rupture distance [km]	6.68	8.95
Horizontal component	North	North
Horizontal PGA [g]	0.254	0.310
Vertical PGA [g]	0.315	0.181

In the next sections, each step of the incremental dynamic test will be identified by the three letters of the signal label, i.e. "EMN" or "CIN", followed by the percentage of acceleration amplitude scaling. The suffixes "ISO", "FIX", or "FIX-Z" identify the base-isolated test series, the fixed-base one with only horizontal input, and the fixed-based one with also the vertical component, respectively.

4. Experimental outcomes

4.1 Isolation system response

Fig. 6a shows the trajectories recorded for each of the four KSJ isolators during the highest amplitude run CIN250%-ISO. A pendulum-type motion with variable curvature was obtained, in good agreement with the analytical prediction for the loaded device. The maximum horizontal displacement of about 80 mm corresponded to an upward displacement of nearly 4 mm on isolators no. 1 and 2, which started from the exact at-rest position, as correctly anticipated by the kinematic analysis. The trajectory of isolators no. 3 and 4 was slightly shifted to the left, probably due to some misalignment during assemblage of the setup, which resulted in minor initial displacements. The analytical model did not catch the isolator downward settlement, which progressively cumulated up to residual vertical displacements ranging between 0.2 mm and 0.4 mm after EMN250%-ISO. This effect tended to stabilize, however, with residual settlements varying between 0.2 mm and 0.6 mm at the end of CIN250%-ISO. Plays and adjustments of the pinned connections are likely at the origin of these settlements.

Fig. 6b illustrates the hysteretic lateral force-displacement response obtained for the entire system during test run CIN250%-ISO. The loops resemble those obtained for friction-pendulum devices, except for their variable slope due to the KSJ variable-curvature trajectory. The loop tangent becomes horizontal (zero lateral stiffness) at a lateral displacement of about 60 mm, where the trajectories of Fig. 6a approach straight lines (zero curvature), confirming the analytical prediction. The loop width measured along the force (vertical) direction represents the contribution of friction within pinned joints. In particular, a width of about 12 kN indicates a frictional resistance of 6 kN. If the friction effects are subtracted from the loops, the experimental results confirm the analytical prediction, with a restoring force of about 15 kN for 80 mm of maximum lateral displacement.

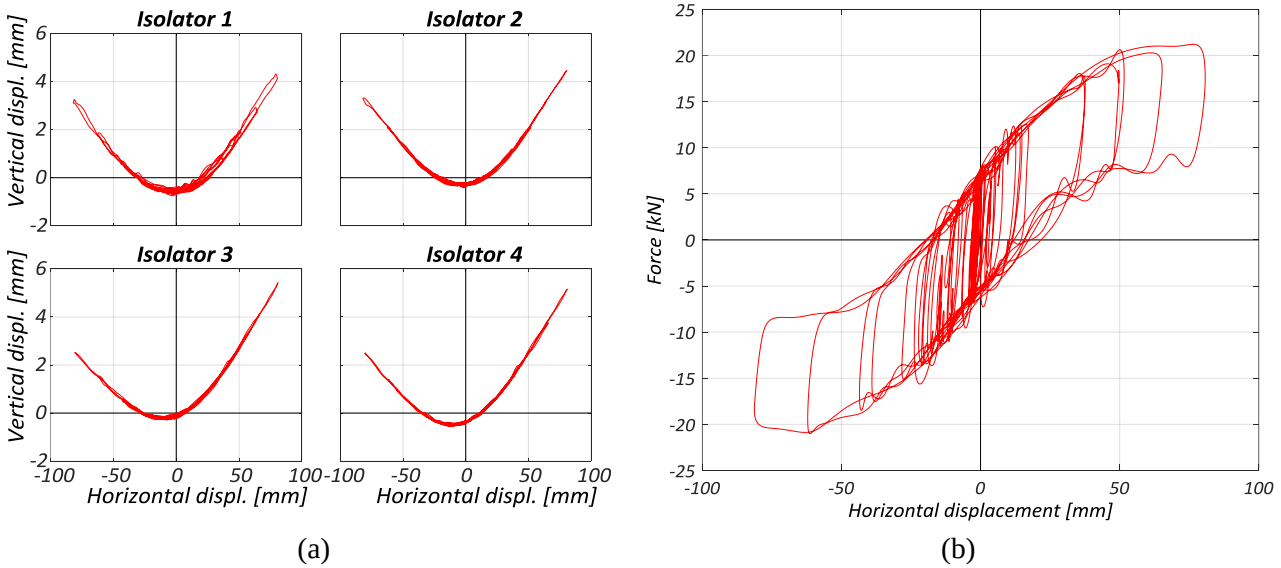

(a) (b)

Fig. 6 – Experimental response of the KSJ prototype during test run CIN250%-ISO: (a) trajectories of individual devices; (b) overall lateral hysteretic response for a superstructure weight of 205 kN.

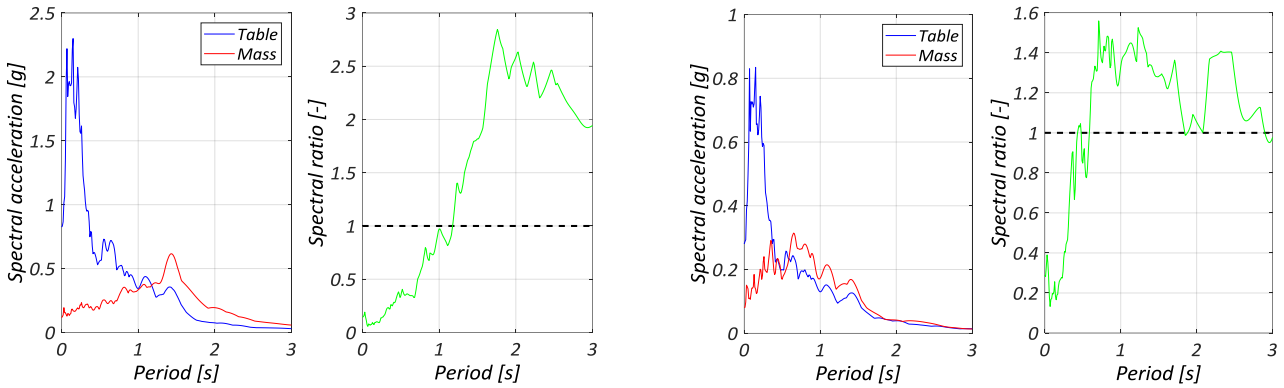

(a) (b)

Fig. 7 – Isolation effectiveness and response spectra: (a) test run CIN250%-ISO; (b) test run CIN100%-ISO.

The effectiveness of the proposed isolation system was evaluated in terms of elastic response spectra at 5% viscous damping ratio. Response spectra were calculated for two acceleration signals: (i) the one recorded by the sensor on the shake-table, and (ii) the average of those recorded by the two accelerometers attached to the RC main mass. The ratio of the second to the first spectral ordinates informs about the reduction or amplification of the demand imposed to the superstructure, quantifying the effectiveness of the isolation system.

Fig. 7 shows that under the CIN250%-ISO input the isolators reduce the spectral ordinates up to periods of about 1.0 s. Instead, they amplify the demand on longer-period oscillators, with maximum amplification around 1.7 s. This corresponds to the average isolated period of $T_b \approx 1.8$ s analytically predicted for a maximum displacement of 80 mm, [22]. According to the recommendations of the Italian building code [24], this isolation system could be adopted for superstructures with fundamental period $T_s \leq 0.33\ T_b = 0.6$ s, which in fact would fall within the spectral-reduction range. It is noteworthy that the average period of the isolation system depends on the lateral displacement underwent by the KSJ devices: smaller displacements result in smaller average radius of curvature of the trajectory, and consequently in shorter average isolated periods. Consequently, also the spectral-reduction period range depends on the displacement demand on the KSJ isolators: for lower-intensity input motions, which impose smaller displacements on the isolators, the range becomes narrower. For example, Fig. 7 shows that the spectral-reduction range under CIN100%-ISO is limited to a maximum of 0.4 s.

4.2 Non-structural component response

Incremental dynamic test (IDT) curves were derived for the rocking marble blocks and for the museum showcase (Fig. 8 and Fig. 9). The recorded horizontal peak ground acceleration (PGA) was chosen as intensity measure for all non-structural components. The maximum lateral displacement, normalized with respect to the critical value at onset of static instability, was taken as engineering demand parameter for the rocking blocks. The maximum top acceleration amplification, with respect to the shake-table acceleration, was used for the showcase instead. Safety steel cables restrained the free-rocking block, limiting its displacement to 80% of the critical one to avoid damage to nearby components, as shown by the dashed lines on Fig. 8 and Fig. 9.

Seismic isolation was particularly effective at preventing instability of the one-side-rocking block all the way to PGA of 0.82 g (Fig. 8a and Fig. 9a). That same block overcame its critical displacement in fixed-base conditions during the EMN200%-FIX and EMN175%-FIX-Z tests, for PGA of 0.45 g and 0.43 g, respectively. Isolation was less beneficial for the free-rocking block (Fig. 8b and Fig. 9b), despite some displacement demand reduction under the same PGA. In particular, this block engaged the safety restraint system in isolated configuration during test run EMN200%-ISO with PGA of 0.49 g. It is noteworthy that

this PGA was not reached when scaling the EMN record in fixed-base conditions; moreover imperfections at the base of the free-rocking block resulted in vibrations under PGA lower than the theoretical rocking activation acceleration of 0.2 g. Generally, the EMN signal appeared more demanding than the CIN record for the rocking elements of the test setup, due to its frequency content. No evident effects were observed related to the application of the vertical excitation component.

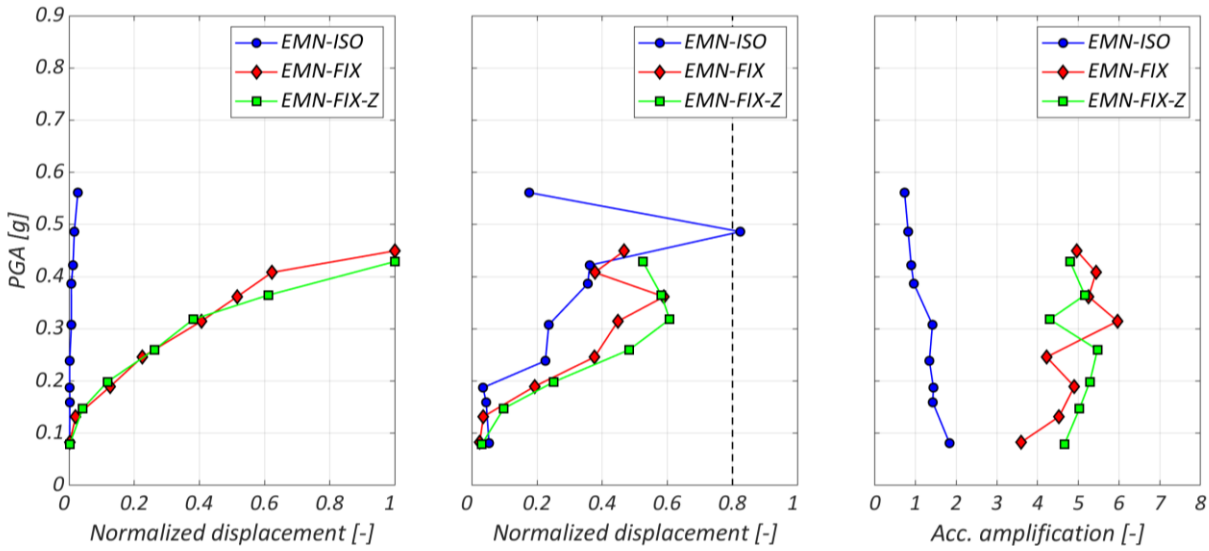

(a) (b) (c)

Fig. 8 – Non-structural component IDT curves under EMN scaled input: (a) one-side-rocking block; (b) free-rocking block; (c) museum showcase.

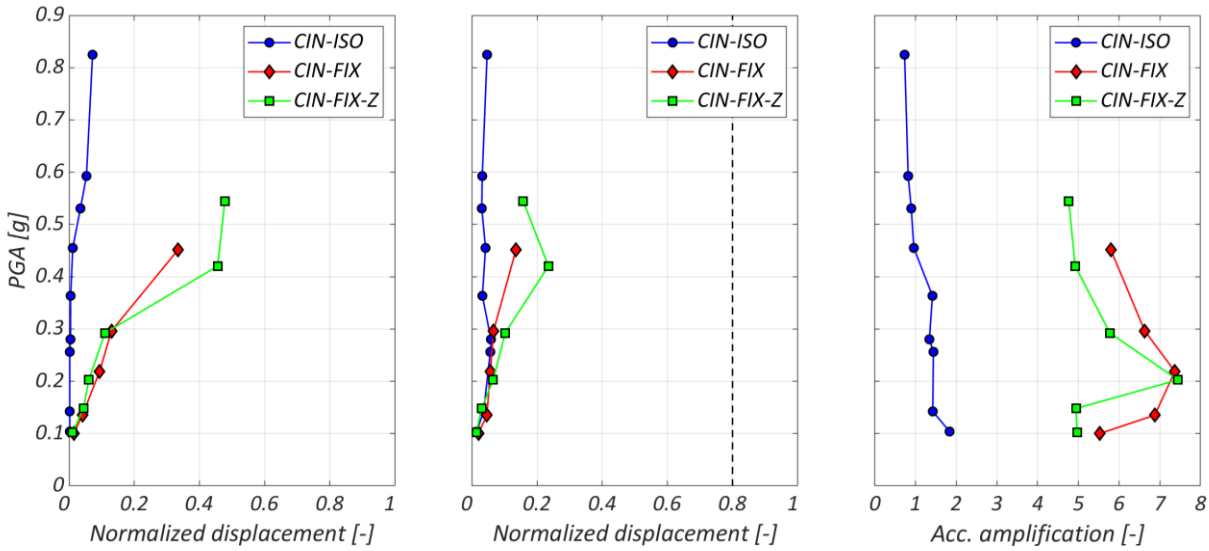

(a) (b) (c)

Fig. 9 – Non-structural component IDT curves under CIN scaled input: (a) one-side-rocking block; (b) free-rocking block; (c) museum showcase.

The isolation system reduced significantly the acceleration amplification of the museum showcase (Fig. 8c and Fig. 9c). Similar trends were observed using both signals. More specifically, seismic isolation allowed decreasing the acceleration by a factor of 3 to 6, depending on the intensity of the input signal. Application of the vertical acceleration input in fixed-base configuration did not induce any appreciable variation in the showcase response. The behavior of the Michelangelo's David small-scale replica was less influenced by isolation: the statue fell during test runs EMN125%-ISO and EMN125%-FIX, for PGA slightly higher than 0.3 g in both cases. Adding the vertical excitation component had some effect on its behavior, anticipating its fall to PGA of 0.25 g during run EMN100%-FIX-Z.

5. Conclusions

This paper has discussed the experimental response of an innovative seismic isolation device based on a multiple articulated quadrilateral mechanism, named "Kinematic Steel Joint" (KSJ), and its effectiveness at protecting non-structural cultural heritage components from earthquake-induced accelerations. Compared to the isolators currently available on the market, the KSJ solution offers the advantages of competitive fabrication costs, because it consists of simply cut and folded steel sheets with pinned joints, and low-maintenance requirements, if it is made of stainless steel.

The results of an incremental, unidirectional dynamic shake-table test campaign confirmed the behavior of the proposed isolation technology predicted through an analytical formulation. The KSJ isolator applied to the isolated superstructure a restoring force proportional to the slope of the motion trajectory, consisting of upward and lateral displacements with recentering features, similarly to friction pendulum devices. The period of the isolated system was independent of the mass and related to the curvature of the trajectory, which was not constant. However, an average period could be estimated with the equation of a simple gravity pendulum, considering an average radius of curvature at the lateral displacement of interest. The KSJ solution proved to be effective at reducing the seismic demand on the superstructure, over a period range that varies with the displacement demand imposed on the isolators. Finally, the KSJ isolators can provide some energy dissipation thanks to friction at the pinned joints.

The response of two rocking blocks and a museum showcase, mounted above the isolated mass, generally benefitted from the base-isolation system, compared to the fixed-base configuration. Seismic isolation prevented instability of the one-side-rocking block and dramatically reduced the acceleration demand on the showcase by a factor of 3 to 6, depending on the input intensity. The free-rocking block was less sensitive to the seismic protection solution: despite some displacement demand reduction, the block engaged the safety restraints as soon as the PGA increased above the one withstood in fixed-base condition. Tests conducted in fixed-base configuration, with the same horizontal input sequence combined with vertical excitation, resulted in a negligible influence of the latter. The small-scale replica of Michelangelo's David statue, installed inside the showcase, was less sensitive to the presence of an isolation system; however, it was negatively affected by the application of the vertical component, which anticipated its fall from more than 0.3 g of PGA to about 0.25 g.

The results of this preliminary study encourage future development of the KSJ isolator. Further investigations and geometric optimizations will allow to reduce the size of the devices and to obtain lateral displacement ranges and trajectory curvatures compatible with a variety of building and non-structural component configurations. The experimental outcomes have confirmed the importance of protecting cultural heritage assets from earthquake-induced accelerations and the effectiveness of seismic isolation for this purpose.

6. Acknowledgements

The authors would like to thank Kyneprox S.r.l. for the financial and material collaboration in the development and testing of the proposed technology. The financial support to the experimental campaign provided by the EUCENTRE Foundation, within the project Mobartech (Regione Lombardia), and by

Goppion S.p.A., is gratefully acknowledged. The valuable contributions of G. Ausenda, G.C. De Sanctis, and the EUCENTRE Foundation laboratory staff are also duly appreciated.

7. References

[1] Guerrini G, Restrepo JI, Massari M, Vervelidis A (2015). Seismic behavior of posttensioned self-centering precast concrete dual-shell steel columns. *Journal of Structural Engineering (ASCE)*, **141**(4), 04014115. DOI: 10.1061/(ASCE)ST.1943-541X.0001054

[2] Ding D, Arnlod C, et al. (1990). Architecture, building contents, and building systems. *Earthquake Spectra*, **6**(1-suppl), 339-377. DOI: 10.1193/1.1585607

[3] Filiatrault A, Sullivan T (2014). Performance-based seismic design of nonstructural building component. *Earthquake Engineering and Engineering Vibrations*, **13**(1-suppl), 17-46. DOI: 10.1007/s11803-014-0238-9

[4] Di Sarno L, Petrone C, Magliulo G, Manfredi G (2015). Dynamic properties of typical consultation room medical components. *Engineering Structures*, **100**, 442-454. DOI: 10.1016/j.engstruct.2015.06.036

[5] Spyrakos CC, Maniatakis CA, Taflampas IM (2017). Application of predictive models to assess failure of museum artifacts under seismic loads. *Journal of Cultural Heritage*, **23**, 11-21. DOI: 10.1016/j.culher.2016.10.001

[6] Fragiadakis M, Kolokytha M, Diamantopoulos S (2017). Seismic risk assessment of rocking building contents of multistorey buildings. *Procedia Engineering*, **199**, 3534-3539. DOI: 10.1016/j.proeng.2017.09.507

[7] Kelly TE (2001). *Base Isolation of Structures - Design Guidelines*. Holmes Consulting Group Ltd, Wellington, New Zealand.

[8] Sorace S, Terenzi G (2015). Seismic performance assessment and base-isolated floor protection of statues exhibited in museum halls. *Bulletin of Earthquake Engineering*, **13**(6), 1873-1892. DOI: 10.1007/s10518-014-9680-3

[9] Gidaris I, Taflanidis AA, Lopez-Garcia D, Mavroeidis GP (2016). Multi-objective riskinformed design of floor isolation systems. Earthquake Engineering & Structural Dynamics, **45**(8), 1293-1313. DOI: 10.1002/eqe.2708

[10] Caliò I, Marletta M (2003). Passive control of the seismic rocking response of art objects. *Engineering. Structures*, **25**(8): 1009-1018. DOI: 10.1016/S0141-0296(03)00045-2

[11] Lowry M, Farrar BJ, Armendariz D, Podany J (2007). Protecting collections in the J. Paul Getty Museum from earthquake damage. *WAAC Newsletter*, **29**(3), 16-23.

[12] Vassiliou MF, Makris N (2012). Analysis of the rocking response of rigid blocks standing free on a seismically isolated base. *Earthquake Engineering and Structural Dynamics*, **41**(2), 177-196. DOI: 10.1002/eqe.1124

[13] Baggio S, Berto L, Favaretto T, Saetta A, Vitaliani R (2015). Seismic isolation technique of marble sculptures at the Accademia Gallery in Florence: numerical calibration and simulation modelling. *Bulletin of Earthquake Engineering*, **13**(9), 2719-2744. DOI: 10.1007/s10518-015-9741-2

[14] Chrysostomou CZ, Kyriakides N, Roussis PC, Asteris PG (2015). Emerging technologies and materials for the seismic protection of cultural heritage. In: *Handbook of Research on Seismic Assessment and Rehabilitation of Historic Structures*, Asteris PG and Plevris V, Eds., pp. 576-606, IGI Global. DOI: 10.4018/978-1-4666-8286-3.ch019

[15] Podany J (2017). *When Galleries Shake: Earthquake Damage Mitigation for Museum Collections*. Getty Publications, Los Angeles, CA, USA. ISBN 978-1-60606-522-8

[16] Christopoulos C, Filiatrault A (2006). *Principles of Passive Supplemental Damping and Seismic Isolation*. IUSS Press, Pavia, Italy. ISBN: 88-85701-10-6

[17] Lee DJ (1981). Recent experience in the specification, design, installation, and maintenance of bridge bearings. *Proc. World Congress on Joint Sealing and Bearing Systems for Concrete Structures*, Publication SP-70, Vol. 1, pp. 161-175, American Concrete Institute, Detroit, MI, USA.

[18] Kauschke W, Baigent M (1986). Improvements in the long term durability of bearings in bridges, especially of PTFE slide bearings. *Proc. 2nd World Congress on Joint Sealing and Bearing Systems for Concrete Structures*, Publication SP-94, Vol. 2, pp. 577-612, American Concrete Institute, Detroit, MI, USA.

[19] Clark PW, Kelly JM, Aiken ID (1996). Aging studies of high-damping rubber and lead-rubber seismic isolators. *Proc. 4th U.S.-Japan Workshop on Earthquake Protective Systems for Bridges*, Technical Memorandum No. 3480, 75-89, Public Works Research Institute, Ministry of Construction, Tokyo, Japan.

[20] Morgan T, Whittaker AS, Thompson A (2001). Cyclic behavior of high-damping rubber bearings. *Proc. 5th World Congress on Joints, Bearings and Seismic Systems for Concrete Structures*, Rome, Italy.

[21] Constantinou MC, Whittaker AS, Kalpakidis Y, Fenz DM, Warn GP (2007). *Performance of Seismic Isolation Hardware under Service and Seismic Loading*, Technical report MCEER-07-0012, MCEER, University at Buffalo, The State University of New York, Buffalo, NY, USA.

[22] Guerrini G, Ausenda G, Graziotti F, Penna A (2019). An innovative seismic isolation device based on multiple articulated quadrilateral mechanisms: analytical study and shake-table test. *Proc. 18th ANIDIS Conference*, Ascoli Piceno, Italy.

[23] Luzi L, Pacor F, Puglia R (2019). *Italian Accelerometric Archive v3.0*. Istituto Nazionale di Geofisica e Vulcanologia, Dipartimento della Protezione Civile Nazionale. DOI: 10.13127/itaca.3.0

[24] Ministero delle Infrastrutture e dei Trasporti (MIT) (2019). *Istruzioni per l'Applicazione dell'Aggiornamento delle "Norme Tecniche per le Costruzioni" di cui al Decreto Ministeriale 17 Gennaio 2018*, Circolare 21 gennaio 2019, n.7, C.S.LL.PP., Gazzetta Ufficiale della Repubblica Italiana, Rome, Italy (in Italian).